Shaking Table Tests for Studies of Soil Liquefaction and Soil-Pile Interaction

T.S. Ueng[1]
[1]*Department of Civil Engineering, National Taiwan University, Taipei, Taiwan*
National Center for Research on Earthquake Engineering, Taipei, Taiwan
E-mail: ueng@ntu.edu.tw

ABSTRACT: Physical model tests using a large biaxial laminar shear box on the shaking table at the National Center for Research on Earthquake Engineering (NCREE), Taiwan was conducted to study the liquefaction behavior of saturated sand under one- and multi-directional earthquake shakings. Specimens of clean Vietnam silica sand and Mailiao sand with silt were prepared using specially designed pluviators. Model piles made of steel and aluminum pipes were also placed inside the shear box to evaluate the pile performances and soil-pile interaction within saturated Vietnam sand under shakings. The input shakings included sinusoidal and recorded earthquake accelerations. Pore water pressure changes and accelerations within the soil, displacements and accelerations of the shear box frames, bending and accelerations of the piles at various depths, pile top displacements were measured during the shaking table tests. Settlement of the sand surface after each shaking was also measured. Some analyses using the test results on soil liquefaction, settlement, behavior of pile in saturated sand under shaking were presented.

1. INTRODUCTION

In previous large earthquakes, including the 1999 Taiwan Chi-Chi Earthquake, extensive soil liquefaction occurred and caused severe damage of foundations, lifelines, and water front structures. Excessive settlements, lateral spreading and landslides were also induced by liquefaction (Hwang, et. al, 2003). There are pile foundation failures because of the loss of soil supports and excessive lateral loading. Many studies on soil liquefaction and soil-structure interaction have been performed in order to understand the mechanism of liquefaction and the dynamic responses of foundations in a liquefiable soil under earthquake loading. The results of these studies provide the bases for evaluation of the mitigation methods for liquefaction hazard and aseismic design for structures with pile foundations in a liquefiable ground.

Large soil specimens have been placed and tested on shaking tables that can reproduce the seismic ground shaking under either 1 g or centrifugal conditions (Hushmand et. al, 1988; Taylor et. al, 1995). For a large size physical model, (1) it can better simulate in-situ soil conditions and soil responses, including liquefaction and soil-structure interaction under earthquake shakings; (2) instrumentation can be installed easier with less effects on the responses of soil and structures; and (3) spatial and temporal distributions of responses within the soil specimen can be better measured.

A large-scale laminar biaxial shear box on the shaking table at the National Center for Research on Earthquake Engineering (NCREE) in Taiwan has been developed to test a large soil specimen under two-dimensional earthquake shakings for the study of liquefaction behavior of sand and soil-structure interaction. In the two-dimensional shaking, the loading and the soil movements are multidirectional in the horizontal plane of two (X- and Y-) axes, and they also change with time. Thus, the shaking table tests can better simulate the in situ multidirectional seismic loading on the ground and structures within the soil.

This paper presents the shaking table tests performed at NCREE on large sand specimens with and without model piles and the uses of the test data.

2. LARGE BIAXIAL LAMINAR SHEAR BOX

A soil layer under a level ground surface is usually in a K_o condition, while, during an earthquake, the soil at different depths may move differently in the horizontal plane following the upward shear wave propagation. To provide such flexible but unyielding side boundaries as in the field, laminar simple shear boxes composed of layers of frames are commonly used in the tests. For horizontal two-dimensional earthquake shaking, every layer of the frames should be able to move freely in every direction i.e., multi-directionally, in a horizontal (X-Y) plane following the movement of the soil in the container. This can be accomplished if the frames are allowed to move biaxially in both X- and Y-axes simultaneously. Figure 1 shows schematically the biaxial laminar shear box composed of 15 layers of sliding frames. Each layer consists of two nested frames, an inner frame (1880 mm × 1880 mm) and an outer frame (1940 mm × 2340 mm). Both frames are made of a special aluminum alloy with 30 mm in thickness and 80 mm in height, except the uppermost layer that has a height of 100 mm. These 15 layers of frames are separately supported on the surrounding rigid steel walls with a gap of 20 mm between adjacent layers. A sand specimen of 1880 mm × 1880 mm × 1520 mm can be placed inside the inner frames. A 2-mm thick silicone rubber membrane was placed inside the box to provide a watertight container for saturated soil.

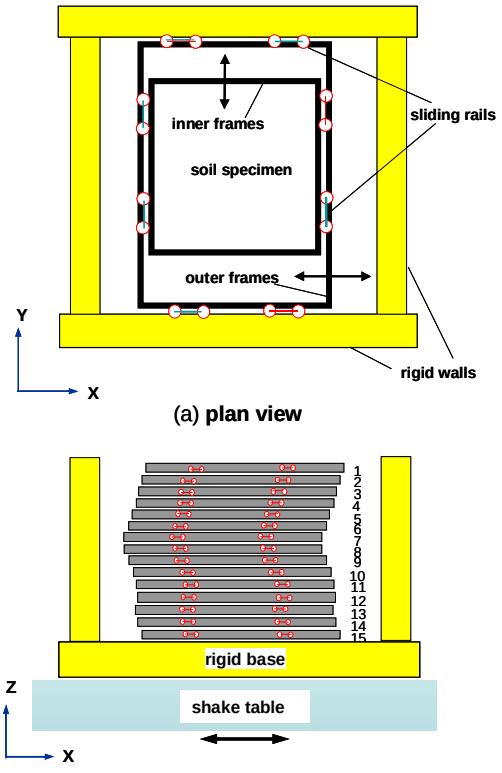

Figure 1. Schematic drawings of the biaxial laminar shear box

Linear guideways consisting of sliding rails and bearing blocks are used to allow an almost frictionless horizontal movement without vertical motions. Each outer frame is supported by the sliding rails built on two opposite sides of the outer rigid walls. The bearing blocks on the outer frame allow its movement in the X direction with minimal friction. Similarly, sliding rails are also provided for each outer frame to support the inner frame of the same layer such that the inner frame can move in the Y direction with respect to the outer frame. With these 15 nested layers of inner and outer frames supported independently on the rigid walls, the soil at each depth can move multidirectionally in the horizontal plane without torsion. Details of the design, manufacturing, and performance of the laminar shear box can be found in Ueng et. al, 2001; 2003; 2006b.

3. SAND SPECIMENS

Vietnam sand and Mailiao sand were used in the shaking tests. Vietnam sand is a commercially available clean fine silica sand while Mailiao sand is a typical soil in the reclamation industrial sites in the western coastal area of Taiwan. The grain shape of Mailiao sand is mainly sub-angular and flaky. It is more compressible and friable than silica sand. Mailiao sand at site contains a wide range of fines from about 5 % up to 80 %, mostly 8–30 % in the shallow depth (< 15 m) (Chen and Huang, 1997). The silt content of the sand obtained for this study is about 6–9 %. The representative grain size distributions of the tested sands are shown in Figure 2. The maximum and minimum void ratios for Vietnam sand are 0.887~0.912 and 0.569~0.610 and those for Mailiao sand with silt are 1.162 and 0.586, respectively.

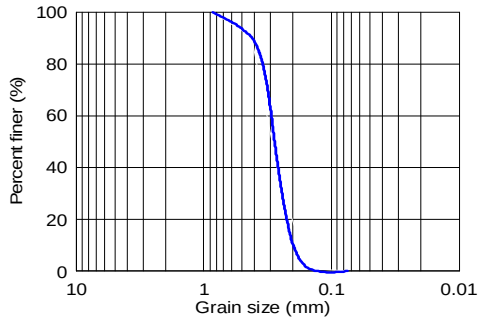

(a) Vietnam sand

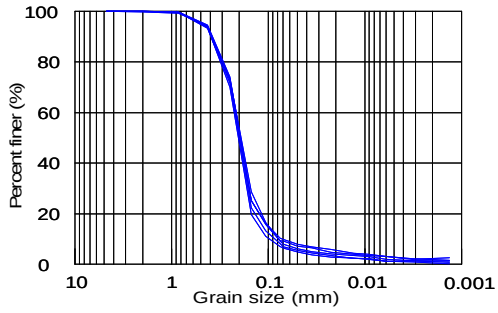

(b) Mailiao sand

Figure 2. Grain size distributions of tested sands

For Vietnam sand, the large specimen inside the shear box was prepared using a specially designed pluviator as shown schematically in Fig. 3(a) (Ueng et. al, 2006b). The dry sand, about 7 Mg in mass, was rained down in one stage into the shear box filled with water to a pre-calculated depth. For Mailiao sand with silt, due to the moist clumpy condition of the natural soil with an average water content of 7.2 %, a different device, as shown in Fig. 3(b), was developed to prepare the large specimen into the laminar shear box by using the staged sedimentation method (Ueng et. al, 2008b). In each stage, approximate 1.0 Mg of sand was dropped into the shear box from the pluviator by opening the bottom vanes about 30 minutes after the previous stage. It took seven stages to complete a Mailiao sand specimen of about 1.350 m in height in this study. The uniformity and density of the sand specimen were evaluated by undisturbed sampling from the shear box after pluviation of the sand. The saturation of the specimens was checked by measuring P-wave velocity across the specimen horizontally at different depths. A small steel ball hit the sand specimen at the 20-mm gaps between the frames and the arrival times of the P-wave were measured using the accelerometers close to the hitting point and across the specimen. The results indicated that the sample was well-saturated and rather uniform in both density and fines content.

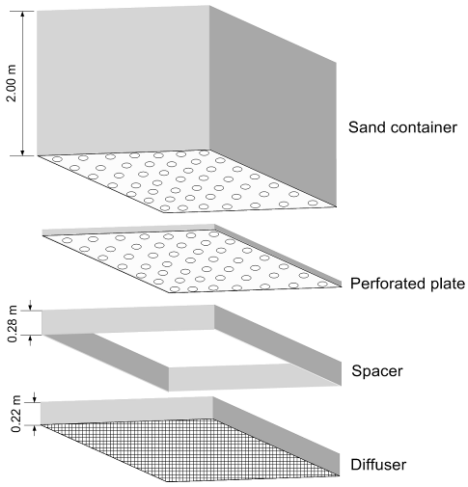

(a) Vietnam sand

(b) Mailiao sand

Figure 3. Pluviators for specimen preparation

4. MODEL PILES

Two different types of model piles were used in the shaking table tests. One was made of a stainless steel pipe, 1.50 m in length, with an outer diameter of 101.6 mm, a wall thickness of 3 mm and a flexural rigidity, EI, of 186.0 kN-m^2; the other was made of an aluminum alloy pipe, 1.60 m in length, with the same diameter and wall thickness and EI = 77.6 kN-m^2. Strain gauges and accelerometers were placed at different locations to respectively measure bending strains and accelerations along the pile. The pile was fixed at the bottom of the shear box to simulate the condition of a pile foundation embedded in rock or within a firm soil stratum. A rigid steel adapter (15.3 kg in mass) for application of lateral force was fixed to the top of the steel pile, while up to 6 steel disks, each with 37.10 kg in mass, were fixed to the top of the aluminum pile to simulate the superstructure of various masses. The model pile with instrumentation inside the shear box was set up before preparation of the sand specimen, as shown in Fig. 4.

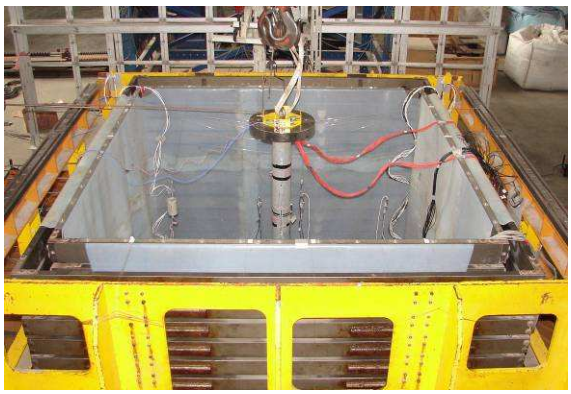

Figure 4. The instrumented aluminum pipe inside the shear box with one steel disk on the top

5. INSTRUMENTATION

To obtain the movements of 15 layers of inner and outer frames at different depths of the laminar shear box and the responses of the sand specimen during shaking tests, magnetostriction-type linear displacement transducers (LDT) and accelerometers were placed at various locations and heights on the outside rigid walls, the outer frames for X-direction motions, and the inner frames for Y-direction motions. Figure 5 shows the layout of the instrumentation on the shear box.

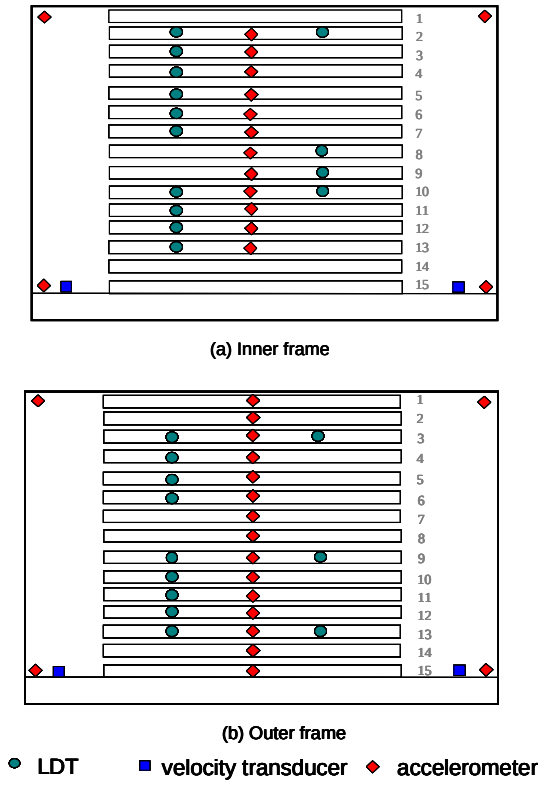

Figure 5. Instrumentation on frames of the shear box

For the build-up and dissipation of the pore water pressures and accelerations in the sand specimen, mini-piezometers and mini-accelerometers, in both X and Y directions, were installed inside the box at different locations and depths (Fig. 6). Piezometers and accelerometers were also placed near the model pile for evaluation of the soil-pile interaction during model pile tests. Additional couple sensors capable of measuring the pore pressure and acceleration at the same location and tactile sensors were installed for evaluation of the applicability of these instruments. These transducers were positioned with thin fishing lines before placing the sand into the shear box. These fishing lines were cut prior to the shaking tests.

Two settlement plates (180 mm in diameter) connected with LDTs were placed to observe the sand surface settlements during shakings.

Two LDTs were mounted to the reference frames outside the shaking table to measure the displacements of the pile top in X and Y directions. Resistance-type stain gauges were placed on the pile surface to measure bending strains of the model pile at 10 different depths with 15 cm in spacing along the pile axis. At each depth, two pairs of stain gauges were mounted on opposite sides of the pile in X and Y directions. Vertical acceleration arrays were also set up along the model pile to measure accelerations of the pile in both X and Y directions. Figure 6 is the layout of instrumentation on the model pile and within the sand specimen.

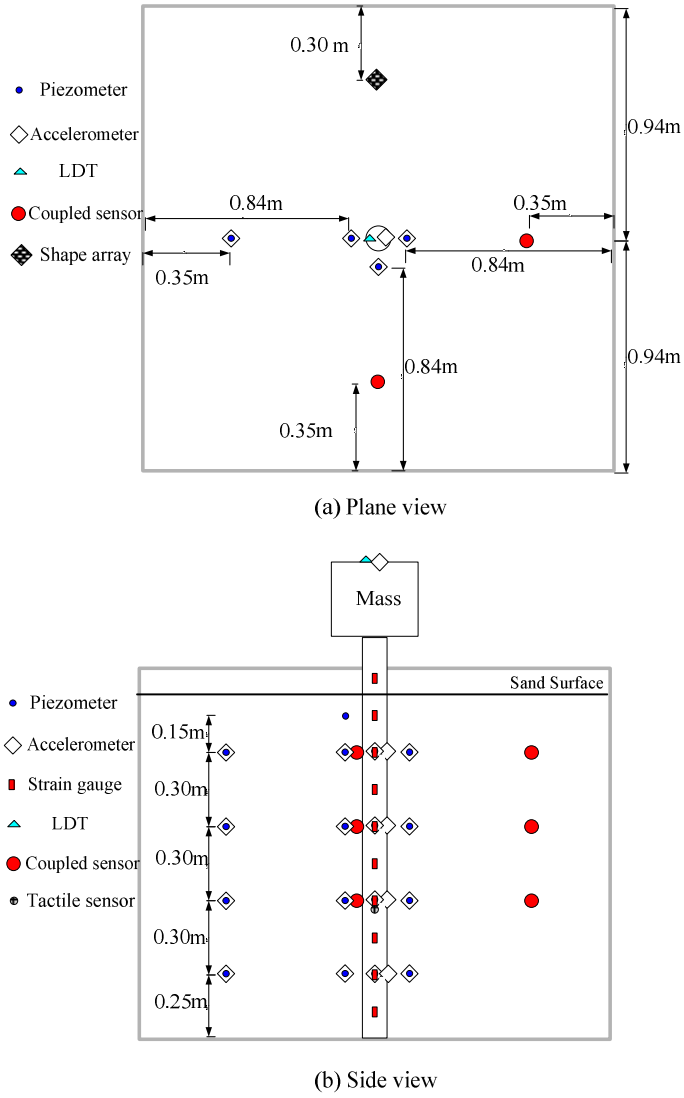

Figure 6. Instrumentation on the pile and within the sand specimen

6. SHAKING TABLE TESTS

Starting from August 2002, numerous shaking table tests have been conducted on the sand specimens, with and without the model piles, in the biaxial laminar shear box at NCREE. They included liquefaction tests to study ground responses and liquefaction behavior of the sand specimen, and model pile tests to evaluate the pile behaviors and soil-pile interactions under shakings.

6.1 Liquefaction Tests

Series of shaking table tests on the Vietnam sand and Mailiao sand

specimens were performed to observe the pore water pressure generations and deformations of the sand specimens. Various one- and multi-directional input motions were imposed by the shaking table. The input motions included sinusoidal (1 Hz, 2 Hz, 4 Hz and 8 Hz) accelerations, with amplitudes (A_{max}) from 0.03g to 0.15g in X and/or Y directions. In the two-dimensional (multidirectional) shaking, there is a 90° phase difference between the input acceleration in X and Y directions, i.e., a circular or ellipse motion was applied. The acceleration, full and reduced amplitudes, recorded at seismograph stations in Chi-Chi Earthquake, Kobe Earthquake and Loma Prieta Earthquake were also imposed in X (N-S) and Y (E-W) directions. In two of the shaking tests, a surcharge of 2860 kg was also placed on top of the Vietnam sand specimen to simulate an about 3-m overlying soil layer.

The outer frames for X-direction motions and the inner frames for Y-direction motions at every depth of the laminar shear box were recorded during shaking using displacement transducers and accelerometers to evaluate the responses and liquefaction of the sand specimen. The accelerations in X and Y directions at various locations and depths of the specimen were also measured with mini-accelerometers. Pore water pressure changes inside the sand specimen were measured continuously until sometime after the end of shaking to observe the generation and dissipation of the pore water pressures. Two settlement plates were also placed to observe the surface settlements during shaking tests. The height of the sand surface was measured manually after each shaking that the settlement of the sand specimen can be calculated. Figure 7 shows the laminar shear box with instrumentation on the shaking table prior to shaking tests. Soil samples were taken using short thin-walled cylinders at different depths after completion of the shaking tests to obtain the densities of the sand specimen.

Figure 7. Mailiao sand specimen in the shear box on shaking table

6.2 Model Pile Tests

In the model pile tests, only clean Vietnam sand was used for the large sand specimen in the shear box.

The lateral load tests on the steel model pile with and without sand were performed under static and cyclic loading by an actuator fixed on the reaction wall at NRCEE (Fig. 8). The input motions of cyclic loading included sinusoidal displacements with amplitudes ranging from 1 mm to 5 mm and frequencies of 0.5 Hz, 1 Hz and 2 Hz. The dial gages, strain gages and piezometers were installed at various locations to measure the responses of the pile and soil under different loading conditions. The height of the sand surface after each loading test was measured to calculate the settlement and density of the sand specimen.

Shaking table tests were first conducted on each model pile without sand specimen to evaluate the dynamic characteristics of the model pile itself. Sinusoidal and white noise accelerations with amplitudes from 0.03 to 0.075 g were applied in X and Y directions. The model pile within the saturated sand specimen was then tested under one- and multi-directional sinusoidal (1~24 Hz) and recorded earthquake accelerations with amplitudes ranging from 0.03 to 0.25 g. White noise accelerations were also applied in both X and Y directions to investigate the behaviors of the model pile and the sand specimen with amplitude of 0.03 g. Figure 9 shows a shaking table test of the aluminum model pile with 6 steel disks on its top in the sand specimen.

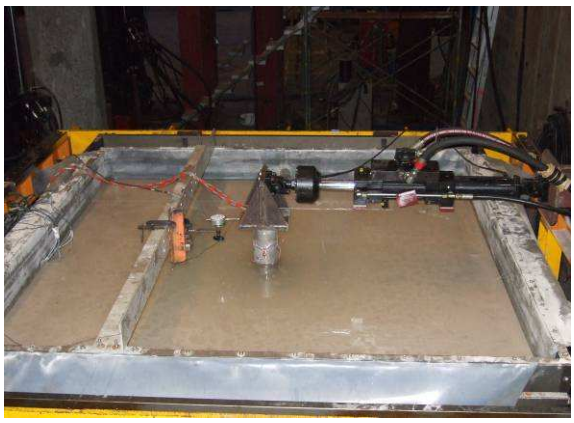

Figure 8. Lateral load test on the steel model pile

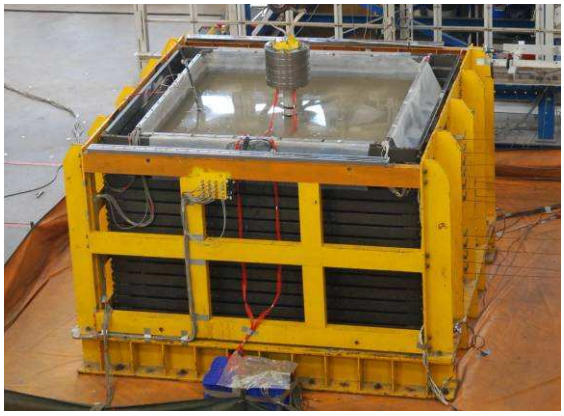

Figure 9. Shaking table test on the aluminum model pile in saturated sand

During every shaking test, pile top displacements, strains and accelerations at different depths on the pile, and pore water pressures and accelerations in the sand specimen (near field and far field) were measured. Besides, the frame movements at different depths of the laminar shear box were also recorded to evaluate the responses and liquefaction of the sand specimen. Pore water pressures inside the sand specimen were measured continuously until sometime after the end of shaking to observe the generation and dissipation of the pore water pressures. The height of the sand surface after each shaking was obtained for the settlement and density of the sand specimen.

7. TEST OBSERVATIONS

7.1 Pore Water Pressure and Liquefaction

Immediately before each shaking test, the height of the water level was measured and the water pressure at each piezometer was recorded to determine the initial piezometer position. The water pressure changes at different locations were measured during shaking table tests and liquefaction of sand can be assessed accordingly. The soil is considered liquefied when the excess pore water pressure reaches the initial effective stress (i.e., $r_u = 1.0$) and usually remained at that value afterwards until some time after the shaking ended. Figure 10 shows time histories of the excess pore water pressures measured by piezometers at different depths in the specimen of Vietnam sand during a shaking test. It can be seen that in this shaking test, the sand within the upper ≈ 637 mm of the

specimen was liquefied rapidly when the shaking started. Once the shallow part of soil liquefied, the water pressures at the deeper depths began to reduce due to the pore water pressure transmittal and dissipation caused by drainage of water through the liquefied zone. At some depths, for example, 483 mm below sand surface, originally liquefied sand became non-liquefied again before the end of shaking.

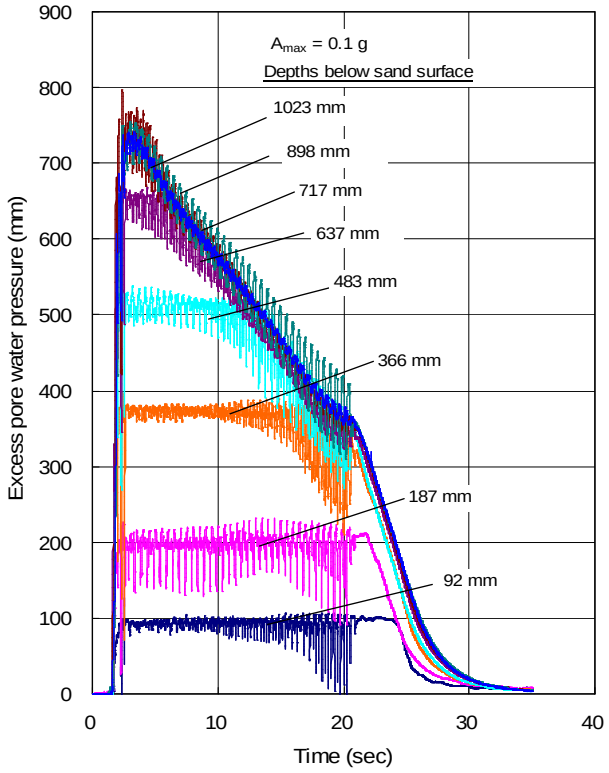

Figure 10. Pore water changes at various depths during a shaking test, October 2004

It was observed in the shaking table tests that liquefaction of the sand specimen is more likely under a shaking of greater amplitude, higher frequency, longer duration, and/or multiple directions. The sand specimen often liquefied again even after many previous occurrences of liquefaction which resulted in a higher density of sand. The measurements of water pressures at different depths in the sand specimen also indicated that the sand at a shallower depth was more susceptible to liquefaction than that at a greater depth. In many cases, the shallower soil liquefied without liquefaction of the deeper soil probably due to the mechanism of water pressure transmission as elucidated by Ueng et. al, 2006a; 2007. The liquefaction depth was determined based on the measurements of mini-piezometers in the sand specimen and accelerometers on the inner frames according to the procedures described in Ueng, et al, 2010.

Figure 11 shows the excess pore water pressure distribution along the depth of the specimen at various time during 1-D and 2-D shaking tests. It can be seen that 1-D shaking induced less excess pore pressure and caused a shallower liquefied layer, while the multidirectional shaking caused a deeper liquefaction zone. The excess pore water pressures generated under 1-D and 2-D shakings measured prior to liquefaction during the shaking tests are compared. Generally, the ratio of excess pore water pressure induced by 2-D shaking to that by 1-D shaking ranges approximately from 2.5 to 3.5 according to the results of shaking table tests performed at NCREE.

Sand boil is a well-known feature after liquefaction owing to the expelled water carrying sand particles with it to the ground surface through volcano-like vents. However, this phenomenon was rarely seen in shaking table tests with a uniform saturated specimen of clean sand probably due to its high permeability and uniformity. Sand boils occurred on the surface of the Mailiao sand with silt after liquefaction in the shaking tests. The thin layer (≈1 mm) of a high fines content material on top of the sand specimen when it was prepared by the staged sedimentation method (Ueng et. al, 2008b) was possibly the main reason for this phenomenon. This low permeability layer could hinder the flow of water and dissipation of pore water pressure. When this high fines content layer was scraped off from the surface of the specimen prior to application of shaking, sand boil was not observed at the beginning of the shaking test but reappeared after a thin low-permeability layer was formed by the fines carried up from the specimen during water pressure dissipation.

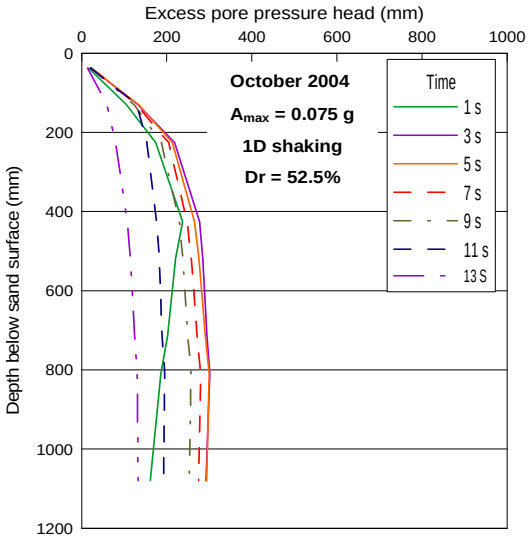

(a) 1-D shaking

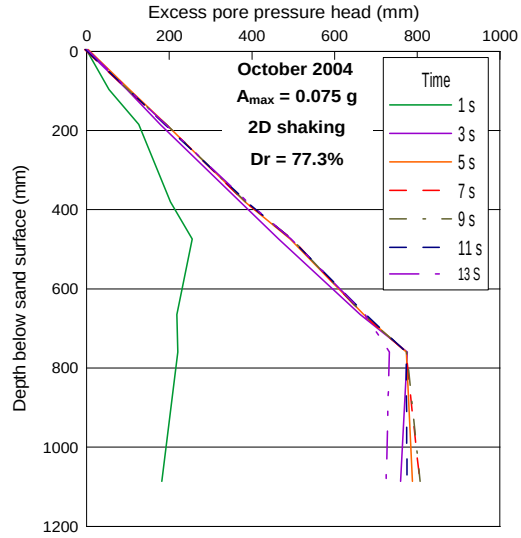

(b) 2-D shaking

Figure 11. Excess pore water pressure distributions versus depth during shaking tests, October 2004

A comparison of pore water pressure changes at five different depths in the specimens of clean Vietnam sand and Mailiao sand with silt during 1-D sinusoidal shaking with an amplitude of A_{max} = 0.1 g is shown in Fig. 12. It can be seen that the excess pore water pressure in Mailiao sand with silt takes a longer time to dissipate than that in Vietnam sand. The piezometer measurements showed that the time of pore water pressure dissipation of Mailiao sand with silt is about 15 times longer than that of clean Vietnam sand. The permeability test results also showed that the ratio of permeability of Vietnam sand to that of Mailiao sand with silt was approximate 15 (Chen, 2007). It illustrates the relation between permeability and rate of pore pressure dissipation after shaking.

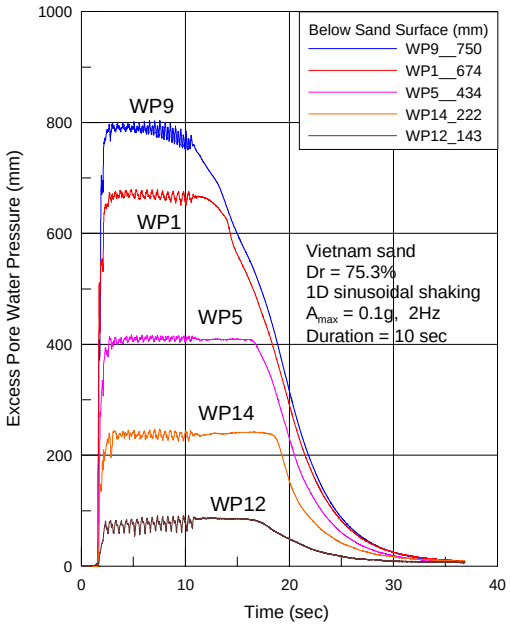

(a) Clean Vietnam sand

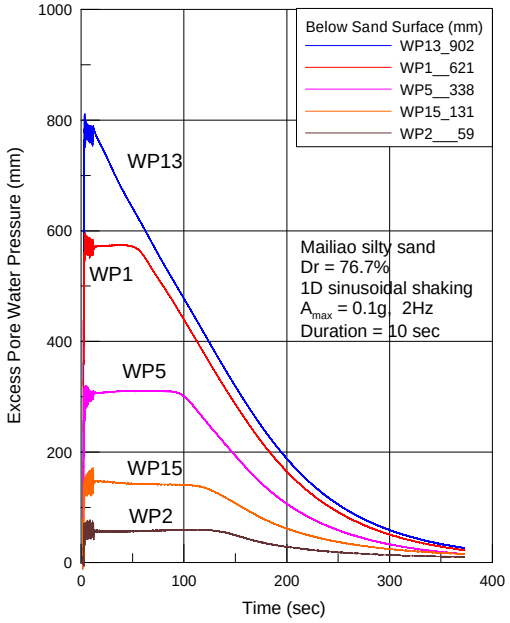

(b) Mailiao sand with silt

Figure 12. Water pressure changes versus time during 1-D shaking

7.2 Settlement after Liquefaction

According to the settlement measurements during and after the shaking tests, the settlements during shakings without liquefaction are very small and insignificant compared with those when there is liquefaction. The settlements resulted from the multidirectional shaking were larger than those under one-directional shaking in both cases of liquefaction and non-liquefaction of the soil.

The volumetric strain of the sand after liquefaction caused by shaking was calculated by dividing the thickness change of the liquefied sand by its depth. With consideration of the liquefaction depth, the test results showed that the volumetric strain after liquefaction, under sinusoidal shakings decreases with relative density of the sand regardless of the amplitude, frequency and directions of shaking. According to the measured displacement of each frame, the maximum shear strain in the specimen ranged between 0.5% and 3.5%. The general trends of volumetric strain changes versus density obtained in this study are similar to those in (Tokimatsu and Seed, 1987). It was also found that the volumetric strain after liquefaction increases with shaking duration. By applying the correlation between shaking duration and earthquake magnitude proposed by Seed and Idriss (Seed and Idriss, 1982), Fig. 13 was obtained for estimating the ground settlements of a liquefied clean sand of different densities subjected to earthquakes of various magnitudes (Ueng et. al, 2010). Results obtained in the shaking table tests subjected to the recorded accelerations in some previous earthquakes are also given on Fig. 13 for comparison. Higher volumetric strains after liquefaction were induced under the Chi-Chi earthquake shakings which exhibit a rather long shaking duration (> 60 s).

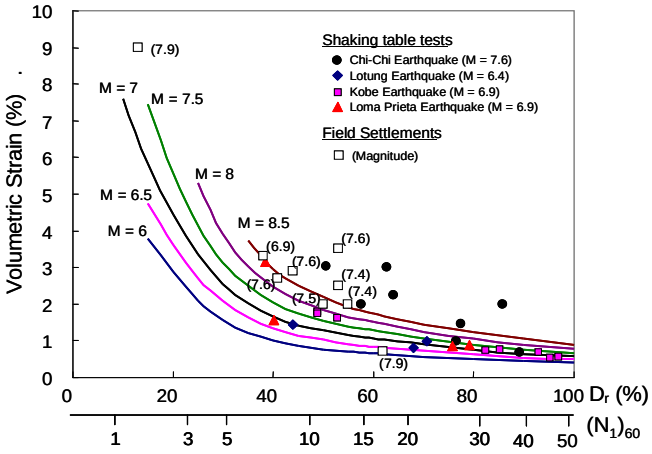

Figure 13. Relations of volumetric strain after liquefaction versus relative density and (N1)60 for various earthquake magnitudes

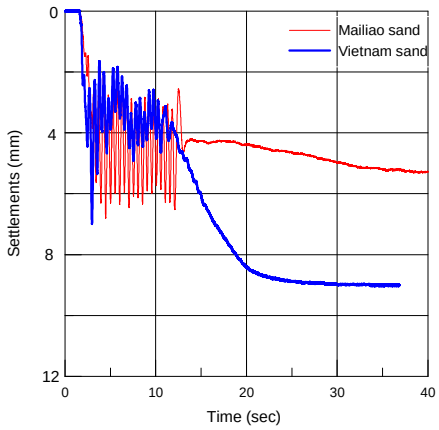

(a)Settlement versus time

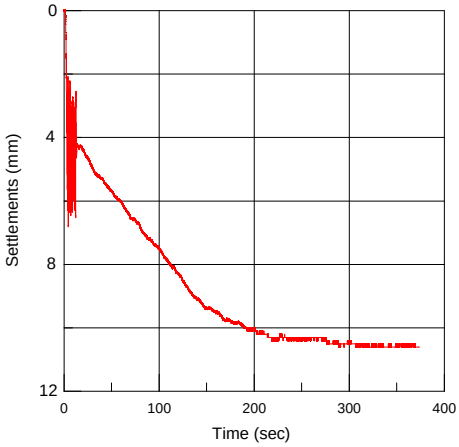

(b) Extended settlement time history for Mailiao sand specimen

Figure 14. Surface settlements versus time for clean Vietnam sand and Mailiao sand with silt specimens during 1-D shaking

Figure 14 shows the measured surface settlements of Vietnam sand and Mailiao sand with silt under the same test conditions as those given in Fig. 12. After dissipation of excess pore water pressure, the final settlements of the Vietnam sand and Mailiao silty sand specimens are 9.0 mm and 10.6 mm, respectively,. The liquefaction depth for Vietnam sand specimen is 1050 mm and that for Mailiao sand specimen is 767 mm. This implies a higher liquefaction resistance for Mailiao sand. With consideration of liquefaction depth, the volumetric strains induced by liquefaction are 0.85 % for Vietnam sand and 1.38 % for Mailiao sand with silt. The greater volumetric strain of Mailiao sand could be attributed to its higher compressibility (Ueng, et. al, 2008a).

7.3 Model pile responses

7.3.1 Lateral loading tests

The flexural rigidity, EI = 186.0 kN-m^2, of the steel model pile was verified with the results of the lateral loading tests on model pile without soil specimen. An equivalent rotational spring was added to take into account the possible rotation at the pile tip at the bottom of the shear box.

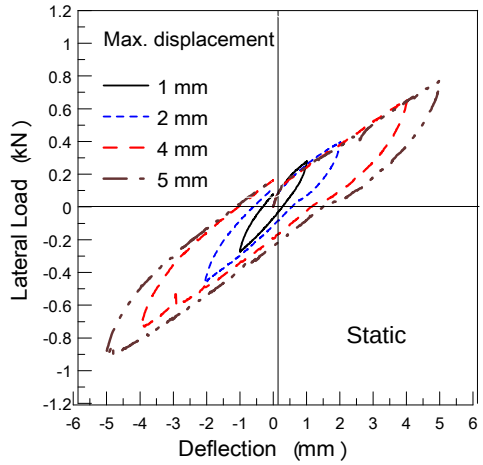

Figure 15. Force-displacement relation for the pile top in lateral load tests on the steel model pile in sand specimen

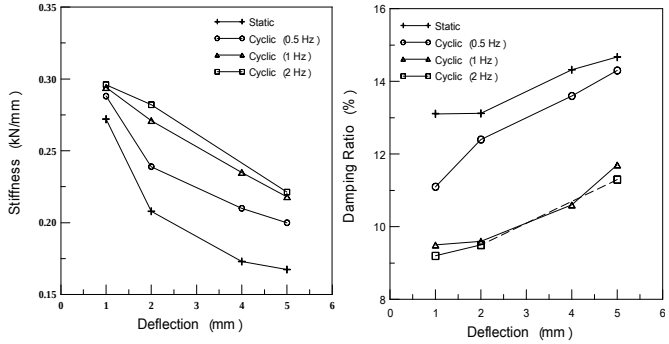

(a) Stiffness (b) Damping ratio

Figure 16. Stiffness and damping ratio of the pile top displacement under cyclic lateral loadings of various frequencies

A typical force-displacement relation for the pile top in a lateral loading test on the steel model pile within the sand specimen is shown in Fig. 15. The equivalent stiffness and damping ratio of the pile top motion were obtained based on the hysteresis force-displacement relation. The stiffness of pile top displacement decreases with increasing deflection and increases with frequency as shown in Fig. 16a. The damping ratio of the model pile increases with increasing deflection and decreases with frequency as shown in Fig. 16b. The p-y curves were also obtained based on the measured pile curvatures at different depths along the pile. The equivalent subgrade reaction modulus according to the p-y curve increases with pile depth. It also increases with loading frequency (Tseng, 2008). These observations suggest that the dynamic soil-pile interaction is affected not only by the pile displacement but also by the rate of pile movement and shaking frequency.

It was observed that the generated excess pore water pressure mainly occurred near the pile perimeter when the model pile subjected to lateral load (Tseng, 2008). Positive excess pore water pressures were generated on the compression side of the pile, while, on the extension side, negative excess pore water pressures were observed.

7.3.2 Under small amplitude shakings

Shaking table tests on both model piles without sand specimen were conducted to evaluate the dynamic characteristics of the model pile. We consider behavior of the model pile in the shear box as a single-degree viscously damped system as shown in Fig. 17. The free vibration motions of the pile top immediately after the end of the input motions were recorded to estimate the natural frequency and damping ratio of the model pile. According to analyses of a series of shaking table tests, the natural frequency of the steel pile with an adapter on the pile top ranged from 13.2 to 13.67 Hz, and the average damping ratio was about 1.6 %. Furthermore, the dynamic characteristics of the model piles can also be evaluated based on the forced vibration of white noise shaking. The amplification curve was derived from the Fourier spectral ratio of the measured acceleration of the pile top to that of the input motion. As shown in Fig. 18, the predominant frequency of the steel pile was identified at 13.62 Hz, which is about the same as that obtained by the other method. Table 1 lists the predominant frequencies of the steel and aluminum model piles according to the test data.

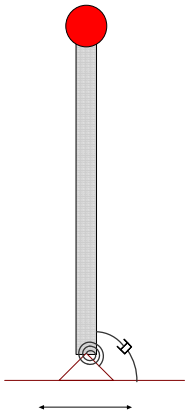

Figure 17. Schematic drawing of the single-degree viscously damped system

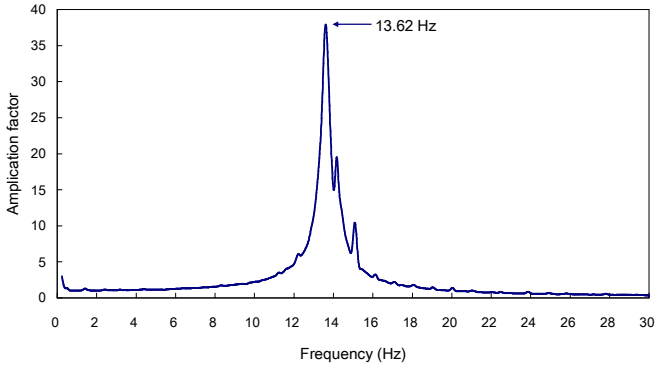

Figure 18. Amplification factor versus frequency for the steel pile from white noise shaking

Table 1. Predominant frequencies of the model piles

Mass on pile top	Predominant frequency, Hz	
	Steel pile	Aluminum pile
No mass	—	23.4
Rigid adapter	13.62	—
1 steel disk	—	5.55
3 steel disks	—	3.11
6 steel disks	—	2.03

The dynamic characteristics of the soil stratum and soil-pile system were evaluated by a series of shaking table tests of small amplitude shakings. Figure 19 shows the amplification factors between the steel pile top and the far-field ground surface under white noise accelerations and sinusoidal vibrations of various frequencies with amplitude of 0.03 g. Results obtained under sinusoidal shakings of various frequencies are also shown in Figure 19. The predominant frequencies of both far-field soil and the pile in soil are nearly the same with a value of about 11.5 Hz. Table 2 lists the predominant frequencies of the soil and the pile in soil of different densities for the case of the steel model pile. It can be seen that the predominant frequencies of soil stratum and pile in soil are almost the same and these frequencies increase with relative density of the sand specimen. This infers that the kinematic force from the soil motion dominates the pile response because of the small inertia force from the superstructure.

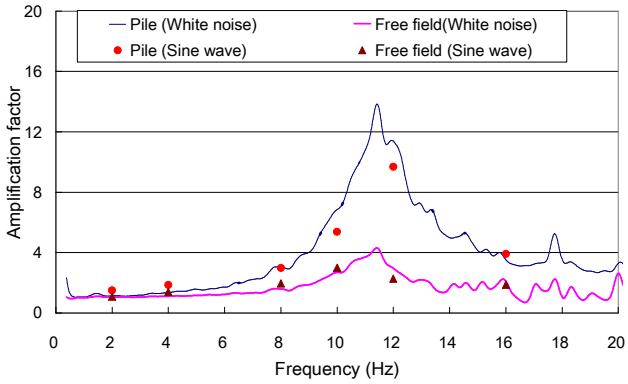

Figure 19. Amplification factor versus frequency for far-field soil and steel pile in soil (Dr = 37.13 %)

Table 2. The predominant frequencies of soil and the steel pile in soil of different densities

Soil density, D_r	Predominant frequency , Hz	
%	Soil	Pile in soil
37.13	11.5	11.5
50.78	12.5	12.38
70.58	12.9	12.9

Table 3 lists the predominant frequencies of the soil stratum and the aluminum pile in soil of various relative densities. It can be seen that, for the model pile without mass and with one steel disk on the top, the predominant frequencies of both soil stratum and pile in soil are almost the same and they increase with relative density of the soil specimen. For the pile with 6 steel disks, the predominant frequency of the pile in soil is significantly lower than that of the far-field soil. Comparing the predominant frequencies of the aluminum pile without and within soil specimen (Table 1 and Table 3, respectively) one can find that, except for the cases without mass on the pile top, the predominant frequencies of the model pile in the soil specimen were higher due to the constraint of soil on the pile. For small inertia force from the superstructure (e.g. no mass or 1 steel disk on the pile top), the pile response was dominated by the kinematic force from the soil motions, but for a larger inertia force (e.g. 6 steel disks on the pile top), the response of pile was mainly governed by the inertia force from the superstructure as depicted in Fig. 20. Therefore, these observations suggest that the inertia force induced by the superstructure plays an important role on the soil-pile interaction.

Table 3. Predominant frequencies of the soil and the aluminum pile in soil of different relative densities

Mass on pile top	Soil density, D_r	Predominant frequency, Hz	
	%	Soil	Pile in soil
No mass	7.5	10.49	10.49
No mass	30.6	11.68	11.7
1 steel disk	31.7	11.8	11.7
1 steel disk	40.5	11.8	11.7
6 steel disks	56.6	13.1	4.88
6 steel disks	64.7	13.2	5.1

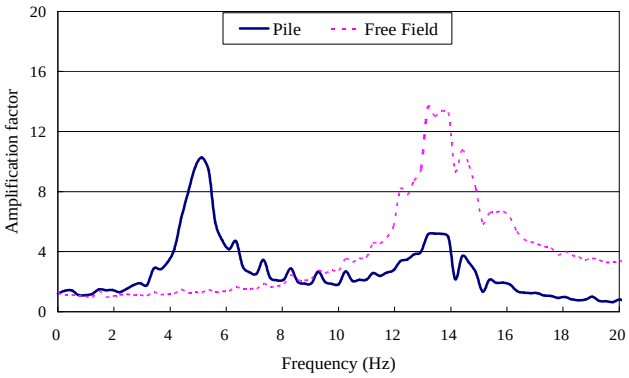

Figure 20. Amplification factor versus frequency for far-field soil and aluminum pile with 6 steel disks (Dr = 64.7 %)

7.3.3 Model piles in liquefiable soil

The performances of both steel and aluminum model piles in liquefied soil during shaking table tests were evaluated based on the measured displacements and accelerations of the piles and accelerations and pore water pressures in the soil (Chen and Ueng, 2010). Figure 21 shows the measured time histories of accelerations and displacements of the aluminum pile with 6 masses on its top and accelerations of the free-field soil and excess pore water pressure ratios (r_u) at various depths in the sand specimen during one-dimensional sinusoidal shaking with frequency of 4 Hz and amplitude of 0.15 g. The whole specimen was fully liquefied at about 3.1 second after shaking started. It was found that the maximum acceleration and displacement of the pile occurred as the sand specimen approached liquefaction. After liquefaction, the pile motions reduced in amplitude and remained steady to smaller vibrations of the same frequency as that of the input motion while the soil motions diminished. It appeared that the soil stiffness vanished and the constraint on the pile was lost when the specimen was fully liquefied. The predominant frequency of the model pile within liquefied soil is estimated at around 2 Hz, which is about the same as that of the model pile without soil (Table 1) (Chen and Ueng, 2010).

8. FURTHER USES OF TESTING DATA AND TESTS

A huge volume of data was obtained in each shaking table test using the biaxial laminar shear box. These data include the responses of the soil specimen and model piles under one- and multidirectional shaking tests with and without soil liquefaction. Only a small portion of the data was interpreted and analyzed by now. Besides those presented in the previous sections, there are many other studies using the test data can be performed for a better understanding of the behavior of soil and soil-pile interaction under earthquake shakings and the development of seismic design of geotechnical structures. Some examples are given as follows.

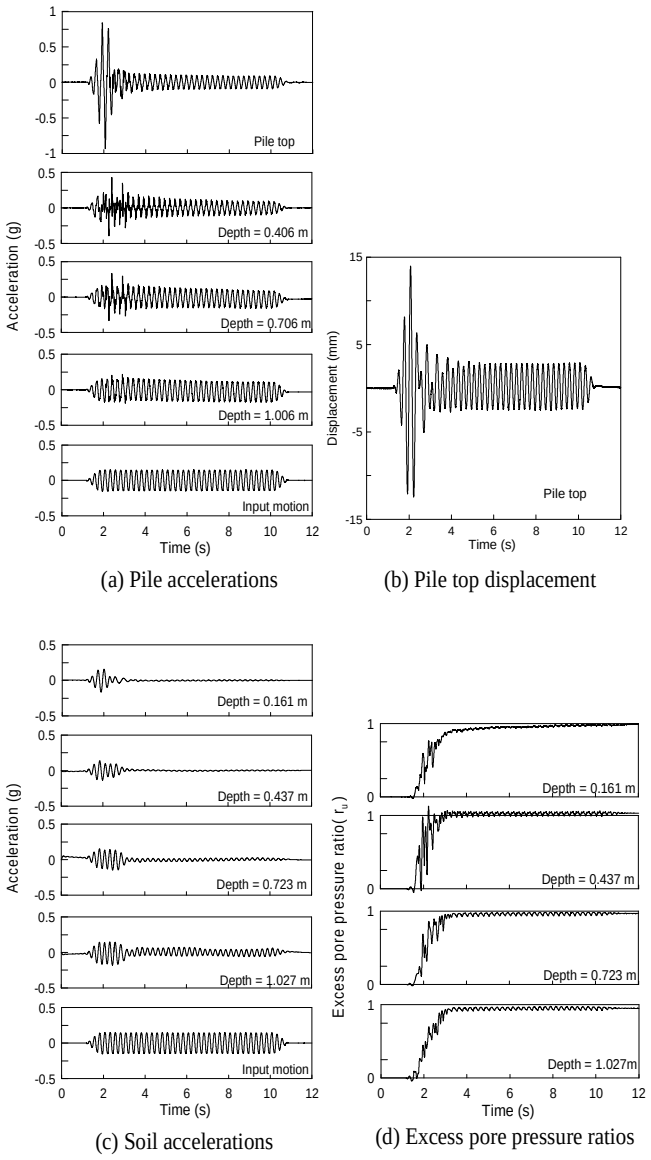

(a) Pile accelerations (b) Pile top displacement

(c) Soil accelerations (d) Excess pore pressure ratios

Figure 21. Time histories of accelerations of the aluminum pile and the free-field soil, pile top displacement and excess pore pressure ratios in the sand specimen (Dr = 68.6 %).

Presently, only limited studies were performed on the effect of 2-D shaking on liquefaction and soil-pile interaction. More quantitative analyses on 2-D effect using the results of shaking table tests with the biaxial shear box, are needed to establish a design guide for 2-D earthquake shakings. In addition, the depth and surface surcharge effect on the soil behavior under shaking should also be looked into using the results of tests with a surcharge on top of the soil specimen.

It was observed in the shaking table tests that the pore water pressure distributions and their changes and the liquefaction behavior of Mailiao sand with silt are different from those of clean silica sand. The behavior of the local soils can be better understood by looking into the test data in more detail, such as pore water pressure generation, dissipation and distribution in the shaking table tests on Mailiao sand with fines.

The soil-pile interaction and pile behavior subjected to shakings, such as dynamic p-y curves, are under investigation using the shaking table test results. The understanding of pore water pressure changes surrounding the pile and its effect on the soil-pile interaction and pile behavior is critically needed. This complex coupling effect between pile motions and pore pressure changes require more careful studies of the test data and further tests.

The shaking table test data may be used for verification of analysis methods and numerica l modeling for ground responses and soil-pile interactions during earthquake shakings. For example, Wu, et al. (Wu et. al, 2009) has developed an identification method for estimating the excitation force acting on the pile with verification by the response measurements in this study.

New measuring devises can be developed and verified by placing them in the soil specimen under various shakings and compare the measurements with those obtained by other conventional instruments. Chang, et al. (Chang et. al, 2007) placed newly developed coupled sensors inside the shear box as shown in Fig. 6 and obtained good results for measuring the coupled shear strain-pore pressure responses of a soil element under multidirectional shakings. Shape array and tactile sensors were also installed and tested for measuring the profiles of displacements and strains within the soil specimen.

Further shaking table tests using the biaxial laminar shear box are planned including tests of pile group and simulation of lateral spreading of liquefied soil of an inclined ground under different shaking conditions as illustrated in Fig. 22. Another biaxial laminar shear box is under construction for testing of multiple bridge foundations on the shaking table simultaneously.

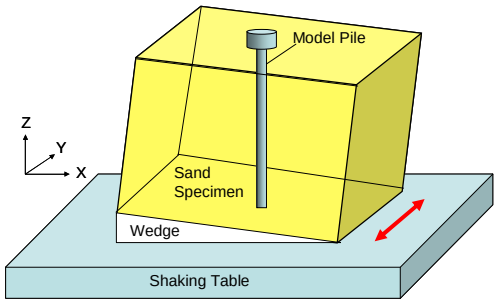

Figure 22. Test on model pile with lateral spreading of soil

9. CONCLUDING REMARKS

A large laminar shear box with a specimen size of 1880 mm × 1880 mm × 1520 mm was developed and manufactured at NCREE. A series of one- and multi-directional shaking table tests were performed on specimens of saturated clean Vietnam sand and Mailiao sand with silt in the shear box to study the responses of the sand under shaking. Special specimen preparation methods were developed for these sands. Shaking table tests were also conducted on steel and aluminum model piles in the biaxial laminar shear box with and without saturated Vietnam sand. The responses of the sand specimen including displacements, accelerations, pore pressure changes and settlements at different locations of the specimen were measured. The displacements, strains and accelerations in X and Y directions at different depths of the model piles were also measured.

Some of the shaking table test results are presented in this paper. The test results showed that a two-dimensional shaking induced higher pore water pressure generation and deeper liquefaction depth than those under the one-dimensional shaking of the same acceleration magnitude. Relations between the volumetric strain after liquefaction and relative density of sand were developed for estimate of the ground settlements after liquefaction during earthquakes. Mailiao sand with silt exhibited a stronger liquefaction resistance but higher volumetric strain after liquefaction than those for clean Vietnam sand. It was found according to analyses of the dynamic responses of the soil-pile system that the behavior of the model pile under shaking was affected by the soil density, the dynamic characteristics of the pile and the surrounding soil, and the mass of the superstructure.

Further tests and analyses of the test data are under way for a better understanding of behaviors of soil liquefaction, soil-pile interaction, and coupling between pore water pressure generation

and pile responses under one- and multi-directional earthquake shakings.

10. ACKNOWLEDGMENT

This study is supported by NCREE and National Science Council, Taiwan. The technical supports and operational assistances from engineers at NCREE in conducting the shaking table tests are greatly appreciated. The assistances in the shaking table testing including large specimen preparation and data acquisition by the faculties and graduate students from National Taiwan University, National Taiwan Ocean University and National Chi Nan University are gratefully acknowledged. The author specially thanks Mr. Chia-Han Chen, a research associate at NCREE and a Ph D student at National Taiwan University, for his efforts in preparation, performance, and data analysis of the shaking table tests.

11. REFERENCES

Chang, W.J., Ueng, T.S., Chen, C.H. and Yang, C.W. "Embedded Instrumentation for Coupled Shear Strain-Pore Pressure Response in Multidirectional Shaking Table test," 4th International Conference on Earthquake Geotechnical Engineering, Thessaloniki, Greece, June 2007, paper No. 1213.

Chen Y.C. "Shaking Table Test on Large Saturated Mailiao Sand Specimens," MS Thesis, Department of Civil Engineering, National Taiwan University, Taipei, Taiwan, 2007. (in Chinese)

Chen, C.H. and Huang F.K. "Liquefaction Risk Evaluation and Microtremor Measurements and Analyses for Reclaimed Soils in the Yunlin Industrial Area," National Center for Research on Earthquake Engineering, Report No. NCREE-97-013, 1997. (in Chinese)

Chen, C.H. and Ueng, T.S. "Behavior of Model Piles in a Liquefiable Soil in Shaking Table Tests," 5th International Conference on Recent Advances in Geotechnical Earthquake Engineering and Soil Dynamics and Symposium in Honor of Professor I.M. Idriss, San Diego, CA, May 2010, paper No. 8.04.

Hushmand, B., Scott R.F., and Crouse, C.B. "Centrifuge Liquefaction Tests in a Laminar Box," Geotechnique, 38, No. 2, 1988, pp. 253–262.

Hwang, J.H., Yang C.W. and Chen C.H. "Investigations on Soil Liquefaction during The Chi-Chi Earthquake," Soils and Foundations, 43, No. 6, 2003, pp. 107–123.

Seed, H.B. and Idriss, I.M. "Ground Motion and Soil Liquefaction during Earthquakes," monograph series, Earthquake Engineering Research Institute, Berkeley, CA, 1982.

Taylor, C.A., Dar, A.R. and Crewe, A.J. "Shaking Table Modelling of Seismic Geotechnical Problems," Proc.10th European Conference on Earthquake Engineering, Duma, 1995, pp. 441–446.

Tokimatsu, K. and Seed, H.B. "Evaluation of Settlements in Sands due to Earthquake Shaking," Journal of Geotechnical Engineering, ASCE, vol. 113, No. 8, 1987, pp. 861–878.

Tseng, Y.C. "Responses of pile in Saturated Sand under Cyclic Lateral Loading,", MS Thesis, Department of Civil Engineering, National Taiwan University, Taipei, Taiwan, 2008. (in Chinese)

Ueng, T.S., Chen, M.H., Wang, M.H. and Ho, W.C. "Large-Scale Shear Box Soil Liquefaction Tests on Shaking Table (I)—Development of the Large Biaxial Shear Box," National Center for Research on Earthquake Engineering, Taiwan. Report No.NCREE-01-011, 2001 (in Chinese).

Ueng, T.S., Chen, C.H., Peng, L.H. and Li, W.C. "Large-Scale Shear Box Soil Liquefaction Tests on Shaking Table (II)—Preparation of Large Sand Specimen and Preliminary Shaking Table Tests," National Center for Research on Earthquake Engineering, Taiwan, Report No.NCREE-03-042, 2003 (in Chinese).

Ueng T.S. "Inference of Behavior of Saturated Sandy Soils during Earthquakes from Laboratory Experiments," Journal of GeoEnginering, TGS, 1, No. 1, 2006a, pp. 1–9.

Ueng, T.S., Wang, M.H., Chen, M.H., Chen, C.H., and Peng, L.H. "A Large Biaxial Shear Box for Shaking Table Tests on Saturated Sand," Geotechnical Testing Journal, ASTM International, 29, No. 1, 2006b, pp. 1–8.

Ueng, T.S. and Chiou, J.S. "Water Pressure Transmission and Soil Liquefaction," Proceedings, 4th International Conference on Earthquake Geotechnical Engineering, Thessaloniki, Greece, June 2007, paper No. 1178.

Ueng, T.S. Chen, C.H., Tsou, C.F. and Chen, Y.C. "Large-scale Shear Box Soil Liquefaction Tests on Shaking Table (IV)—Behavior of Saturated Mailiao Sand Specimen in Shaking Tests," National Center for Research on Earthquake Engineering, Taiwan, Report No.NCREE-08-011, 2008a (in Chinese).

Ueng, T.S., Chen, C.H., Tsou, C.F. and Chen, Y.C. "Shaking Table Test on a Large Specimen of Mailiao Silty Sand," in Proc. GEESD IV, GSP 181 (CD ROM), ASCE, 2008b.

Ueng, T.S., Wu, C.W., Cheng, H.W. and Chen, C.H. "Settlements of Saturated Clean Sand Deposits in Shaking Table Tests," Soil Dynamics and Earthquake Engineering, 30, Issues 1-2, 2010, pp. 50-60.

Wu, A.L., Loh, C.H., Yang, J.N., Weng, J.H., Chen, C.H. and Ueng, T.S. "Input Force Identification: Application to Soil-Pile Interaction," Structural Control and Health Monitoring, 16, No. 2, 2009, pp. 223-240.